

# Can MONDian vector theories explain the cosmic speed up ?

Vincenzo F. Cardone<sup>1,2\*</sup>, Ninfa Radicella<sup>2,3†</sup>

<sup>1</sup>*Dipartimento di Fisica Generale "Amedeo Avogadro", Via Pietro Giuria 1, 10125 - Torino, Italy*

<sup>2</sup>*I.N.F.N. - Sezione di Torino, Via Pietro Giuria 1, 10125 - Torino, Italy and*

<sup>3</sup>*Dipartimento di Fisica, Politecnico di Torino, Corso Duca degli Abruzzi 24, 10129 - Torino, Italy*

Generalized Einstein-Aether vector field models have been shown to provide, in the weak field regime, modifications to gravity which can be reconciled with the successful MOND proposal. Very little is known, however, on the function  $\mathcal{F}(\mathcal{K})$  defining the vector field Lagrangian so that an analysis of the viability of such theories at the cosmological scales has never been performed. As a first step along this route, we rely on the relation between  $\mathcal{F}(\mathcal{K})$  and the MOND interpolating function  $\mu(a/a_0)$  to assign the vector field Lagrangian thus obtaining what we refer to as *MONDian vector models*. Since they are able by construction to recover the MOND successes on galaxy scales, we investigate whether they can also drive the observed accelerated expansion by fitting the models to the Type Ia Supernovae data. Should be this the case, we have a unified framework where both dark energy and dark matter can be seen as different manifestations of a single vector field. It turns out that both MONDian vector models are able to well fit the low redshift data on Type Ia Supernovae, while some tension could be present in the high  $z$  regime.

PACS numbers: 98.80.-k, 98.80.Es, 95.36.+d, 95.36.+x

## I. INTRODUCTION

The old standard cosmological model of a universe full of baryon matter only and regulated by the laws of Einstein General Relativity provided a remarkable picture to consistently explain the background evolution of the universe from the initial singularity up to the present day. Unfortunately, two observational facts then putted in serious trouble this elegant scenario. On the one hand, it turned out that the gravitational field measured on different scales may not be reconciled with what is inferred from baryonic matter only, the most famous example being represented by the flat rotation curves of spiral galaxies [1]. On the other hand, recent data on the Hubble diagram of Type Ia Supernovae (hereafter SNeIa) provided the first evidence for an accelerated expansion [2]. Surprising as it was, the cosmic speed up has been then confirmed by updated SNeIa data [3, 4, 5, 6, 7], the anisotropy spectrum of the Cosmic Microwave Background Radiation (CMBR) as measured by both balloon [8] and satellites [9, 10] experiments, and the data on the large scale clustering of galaxies [11] as estimated from large spectroscopic galaxy surveys.

Both these problems have been traditionally solved by adding new ingredients to the cosmic pie, while leaving unchanged the underlying theory. Cold dark matter (CDM) has been then invoked to fill the gap between the baryon mass (constrained by the Big Bang nucleosynthesis) and what is needed to reproduce the observed gravitational field. Moreover, this mysterious component must not interact with anything but gravitationally so to have escaped any detection notwithstanding the incredible ef-

forts spent up to now to find direct evidence for any dark particle. At the cosmological scales, dark matter still behaves as normal matter so that a further component is needed in order to drive the accelerated expansion. This new actor on the scene must, moreover, have an unusual negative pressure and not cluster on galactic and cluster scales in order to not oppose gravitational clustering. Referred to as dark energy, the nature and nurture of this new term is still debated with the cosmological constant  $\Lambda$  [12] being the simplest candidate. Although added by hand *ad hoc*, the cosmological model comprising both of them and known as  $\Lambda$ CDM is able to fit extremely well the full dataset at disposal [13] thus worthing the name of *concordance model*. Notwithstanding this remarkable success, the  $\Lambda$ CDM is theoretically unappealing because of several well known shortcomings which motivated the search for other dark energy candidates such as quintessence scalar fields [14] and modified gravity theories, either introducing higher dimensions [15] or correcting the gravitational Lagrangian [16, 17].

It is worth noting that both dark matter and dark energy can be avoided if one accepts that the problem is not with what is missing, but rather with how we describe gravity. From this point of view, all the evidences for dark matter and dark energy should be rather seen as evidence that something is wrong with the Newton-Einstein theory of gravity. As a next step, one has therefore to look for a way to modify gravity at both the galactic and cosmological scales possibly finding a unified mechanism explaining phenomena taking place on very different scales such as the flatness of rotation curves and the acceleration of the universe expansion.

Generalized Einstein-Aether theories are one of these proposed mechanisms based on the introduction of dynamical timelike vector field with noncanonical kinetic terms. Such a proposal is not fully new, but builds upon the extensive analysis of standard Einstein-Aether theo-

---

\*winnyenodrac@gmail.com

†ninfa.radicella@polito.it

ries [18] as phenomenological probes of Lorenz violation in quantum gravity. Indeed, the nonvanishing expectation value of the Aether field will dynamically select a preferred frame in the spacetime, namely the one in which the time coordinate basis vector  $\partial_t$  is aligned with the direction of the vector field, thus leading to violation of the Lorenz and gauge invariance. The interest in these models was then renewed after the demonstration [20] that TeVeS, i.e. the fully relativistic and complete MOND theory [19], can be reformulated as a generalized Einstein-Aether theory. Later, it has been shown that it is possible to get a MOND-like behaviour in the weak field regime of vector models [21]. Motivated by these considerations, we explore here the cosmological viability of these theories by suitably setting the vector field Lagrangian in such a way that the successful MOND phenomenology is recovered in the Newtonian limit.

The structure of the paper is as follows. The basic equations and properties of the vector models are described in Sect. II where we also explain how we choose the vector field Lagrangian. Sect. III is devoted to a detailed description of the statistical methodology and the data used to test the models in the low redshift regime with a discussion of the results obtained from the likelihood analysis. A similar test is then presented and discussed in Sect. IV where we add high redshift data to probe this complementary redshift range. Conclusions and perspectives are finally given in Sect. V.

## II. THE MODEL

A general action for a vector field  $\mathbf{A}$  coupled to gravity can be written as

$$S = \int d^4x \sqrt{-g} \left[ \frac{R}{16\pi G_N} + \mathcal{L}(g, A) \right] + S_M \quad (1)$$

where  $G_N$  is the Newton gravitational constant,  $\mathbf{g}$  the metric (with the signature  $-, +, +, +$ ),  $R$  the Ricci scalar and  $S_M$  the matter action. The vector field Lagrangian  $\mathcal{L}$  may be a whatever covariant and local function, but, following [21], we will only consider the case:

$$\mathcal{L}(g, A) = \frac{M^2}{16\pi G_N} \mathcal{F}(\mathcal{K}) + \frac{\lambda(A^\alpha A^\alpha + 1)}{16\pi G_N} \quad (2)$$

where  $\mathcal{F}$  is a generic function of

$$\mathcal{K} = M^{-2} \mathcal{K}^{\alpha\beta}_{\gamma\sigma} \nabla_\alpha A^\gamma \nabla_\beta A^\sigma \quad (3)$$

$$\mathcal{K}^{\alpha\beta}_{\gamma\sigma} = c_1 g^{\alpha\beta} g_{\gamma\sigma} + c_2 \delta^\alpha_\gamma \delta^\beta_\sigma + c_3 \delta^\alpha_\sigma \delta^\beta_\gamma. \quad (4)$$

It is worth noticing that  $\mathcal{K}$  represents all the possible canonical kinetic terms that we introduce in the vector

Lagrangian through the generic function  $\mathcal{F}(\mathcal{K})$  thus allowing to have also a noncanonical contribution by these terms. The  $c_i$  quantities are dimensionless constants, while  $M$  is a scaling mass parameter and  $\lambda$  a nondynamical Lagrange multiplier with dimensions of mass squared.

It is possible to show [21, 22, 23] that the Einstein field equations may still be formally written as

$$G_{\alpha\beta} = \tilde{T}_{\alpha\beta} + 8\pi G_N T_{\alpha\beta}^M \quad (5)$$

with  $G_{\alpha\beta}$  and  $T_{\alpha\beta}^M$  the usual Einstein and matter stress-energy tensors, while  $\tilde{T}_{\alpha\beta}$  contains the terms related to the vector field and some of its derivatives (see, e.g., [21] for its full expression), while the equation of motion for the vector field reads:

$$\nabla_\alpha (\mathcal{F}' J_\beta^\alpha) + \mathcal{F}' y_\beta = 2\lambda A^\gamma \quad (6)$$

with  $\mathcal{F}' = d\mathcal{F}/d\mathcal{K}$  and

$$J_\sigma^\alpha = (\mathcal{K}^{\alpha\beta}_{\sigma\gamma} + \mathcal{K}^{\beta\alpha}_{\gamma\sigma}) \nabla_\beta A^\gamma \quad (7)$$

and defined the functional derivative:

$$y_\beta = \nabla_\sigma A^\eta \nabla_\gamma A^\xi \frac{\delta (\mathcal{K}^{\sigma\gamma}_{\eta\xi})}{\delta A^\beta}. \quad (8)$$

Introducing the flat Robertson-Walker metric in Eq.(5) then gives the modified Friedmann equations which read:

$$\left[ 1 - \alpha \mathcal{K}^{1/2} \frac{d}{d\mathcal{K}} \left( \frac{\mathcal{F}}{\mathcal{K}^{1/2}} \right) \right] H^2 = \frac{8\pi G_N}{3} \rho, \quad (9)$$

$$\frac{d}{dt} \left[ \left( \alpha \frac{d\mathcal{F}}{d\mathcal{K}} - 2 \right) H \right] = 8\pi G_N (\rho + p), \quad (10)$$

where, because of the metric symmetry, it is:

$$\mathcal{K} = 3\alpha \frac{H^2}{M^2} = \frac{3\alpha}{\varepsilon^2} \frac{H^2}{H_0^2}. \quad (11)$$

Here, we have defined two new parameters, namely  $\varepsilon = M/H_0$  and  $\alpha = c_1 + 3c_2 + c_3$ , while  $(\rho, p)$  are the total energy density and pressure of the source terms (matter, radiation, neutrinos, etc.) and  $H = \dot{a}/a$  is the usual Hubble parameter. Hereafter, we will denote derivatives with respect to  $t$  with a dot and to  $\mathcal{K}$  with a prime, and use a subscript "0" to label present day quantities.

It is convenient to rearrange the above equations in a different form. To this end, we first solve Eq.(9) to get:

$$\alpha \mathcal{F}'(\mathcal{K}) = 1 - \frac{\rho(z)}{\rho_{crit} E^2(z)} + \frac{\alpha \mathcal{F}(\mathcal{K})}{2\mathcal{K}} \quad (12)$$

with  $E(z) = H(z)/H_0$  the dimensionless Hubble parameter. Inserting Eq.(12) into Eq.(10) and using

$$\frac{d}{dt} = -(1+z)H_0E(z)\frac{d}{dz}$$

to change variable, one finally gets :

$$\frac{d}{dz} \left\{ \left[ \frac{\varepsilon^2 \mathcal{F}(\mathcal{K})}{6E^2(z)} - \frac{\rho/\rho_{crit}}{E^2(z)} - 1 \right] E^2(z) \right\} = -\frac{3(\rho+p)/\rho_{crit}}{(1+z)E(z)} \quad (13)$$

with  $\rho_{crit} = 3H_0^2/8\pi G_N$  the present day critical density. Let us now assume that the universe is filled by a matter-like term and radiation. Since the vector field is only coupled to gravity, the continuity equation

$$\dot{\rho} + 3H(\rho+p) = 0$$

still holds for both matter and radiation and we can therefore write the rhs of Eq.(13) as

$$\frac{3(\rho+p)/\rho_{crit}}{(1+z)E(z)} = \frac{[3\Omega_M + 4\Omega_r(1+z)](1+z)^2}{E(z)} \quad (14)$$

with  $\Omega_i = \rho_i(z=0)/\rho_{crit}$  the present day density parameter of the  $i$ -th component.

Eqs.(12) - (13) clearly show that a key role in determining the cosmic evolution is played by the functional expression adopted for  $\mathcal{F}(\mathcal{K})$ . A guide to the choice of this quantity is provided by the observation that, in the nonrelativistic regime, the field equations reduce to :

$$\nabla \cdot \left[ \left( 2 + c_1 \frac{d\mathcal{F}}{d\mathcal{K}} \right) \nabla \Phi \right] = 8\pi G_N \rho \quad (15)$$

with

$$\mathcal{K} = -c_1 \frac{|\nabla \Phi|^2}{M^2}, \quad (16)$$

being  $\Phi$  the gravitational potential sourced by the density distribution  $\rho$ . By using the above expression, we get :

$$\nabla \cdot [\mu(|\nabla \Phi|/M)\nabla \Phi] = 8\pi G_N \rho \quad (17)$$

which is the modified Poisson equation for the MOND theory<sup>1</sup>, provided we identify the MOND interpolating function  $\mu(a/a_0)$  with

$$\mu(a/a_0) = \mu(\sqrt{\mathcal{K}}) = 2 + c_1 \frac{d\mathcal{F}}{d\mathcal{K}}. \quad (18)$$

Note that, by this position, the MOND acceleration scale  $a_0$  turns out to be related to the mass scale  $M$  as

$$a_0 = \frac{\varepsilon c H_0}{\sqrt{-c_1}} \iff c_1 = -\left( \frac{\varepsilon c H_0}{a_0} \right)^2, \quad (19)$$

where we have reintroduced the speed of light  $c$ . It is worth noting that such a model thus provides a natural mechanism to explain why one observationally finds that  $a_0 \sim cH_0$  which now emerges as a consequence of the local and cosmological phenomena being different manifestations of the same underlying theory.

Since we know that MOND makes it possible to fit the flat rotation curves of spiral galaxies (see, e.g., [24] and refs. therein), it is reasonable to assume that a viable expression for  $\mathcal{F}(\mathcal{K})$  should lead to the same interpolating function  $\mu(a/a_0)$  which is successfully used on local scales. Two such functions are the *simple form* [25]

$$\mu(x) = \frac{x}{1+x}, \quad (20)$$

and the *standard form* [26]

$$\mu(x) = \frac{x}{\sqrt{1+x^2}}. \quad (21)$$

Although Eq.(21) has been the first proposal to be tested with success [24], recent analyses [25, 27] seem to favour Eq.(20). However, in order to gain further insight on the problem of which interpolating function is better motivated, we will consider both cases contrasting them against data probing radically different scales.

Inserting alternatively Eqs.(20) and (21) into Eq.(18) gives respectively :

$$\mathcal{F}(\mathcal{K}) = -\frac{4}{c_1} \left[ \sqrt{\mathcal{K}} - \ln \left( 1 + \sqrt{\mathcal{K}} \right) \right], \quad (22)$$

$$\mathcal{F}(\mathcal{K}) = -\frac{2}{c_1} \left[ \mathcal{K} - \sqrt{\mathcal{K}(1+\mathcal{K})} + \ln \left( \sqrt{\mathcal{K}} + \sqrt{1+\mathcal{K}} \right) \right]. \quad (23)$$

Hereafter, we will refer to the models assigned by Eqs.(22) and (23) as the *simple* and *standard MONDian vector model* in order to clearly remember that the main ingredient of this kind of cosmological theory is the presence of a vector field with a Lagrangian constructed in such a way to recover the simple or standard MOND interpolating function. Both expressions for  $\mathcal{F}(\mathcal{K})$  depend on  $\sqrt{\mathcal{K}}$  so that it must be  $\alpha > 0$  in the cosmological setting. In the small  $\mathcal{K}$  limit,  $\mathcal{F}(\mathcal{K}) \sim \mathcal{K}$  for both the simple and standard MONDian vector models so that we

<sup>1</sup> Actually, such a modified Poisson equation was proposed for MOND in the framework of the so called *AQUAL* theory [26], one of the first attempts to work out a relativistic MOND theory. AQUAL was later abandoned since it turned out to be unable to account for lensing data without cold dark matter thus being in contrast with the original MOND philosophy.

can use the perturbative analysis in [28] for the Einstein-Aether models to see whether the condition  $\alpha > 0$  is compatible with the constraints on the coefficients  $c_i$ . The requirement that the Hamiltonian for the perturbations is positive definite implies  $c_1 < 0$ , while the constraint  $(c_1 + c_2 + c_3)/c_1 \geq 0$  has to be set in order to avoid tachyonic propagation of spin-0 modes. On the other hand, if we allow superluminal propagations of both spin-0 and spin-2 modes, as supported in [29], we then get that for  $c_2 > 0$  and

$$-(c_1 + 3c_2) \leq c_3 \leq -(c_1 + c_2)$$

it is indeed  $\alpha > 0$  so that we can safely consider the MONDian vector models without violating any constraint on the  $c_i$  coefficients.

### A. The simple MONDian vector model

In order to determine the dynamics for this case, we have to insert Eq.(22) into the master equation (13) and solve with respect to  $E(z)$ . Somewhat surprisingly, after some algebra, we get :

$$\mathcal{Q}[z, E(z)] \times \frac{dE}{dz} = 0$$

with  $\mathcal{Q}[z, E(z)]$  an algebraic function of redshift  $z$ , the dimensionless Hubble parameter  $E(z)$  and the constant parameter of the model. Since we know that the universe is expanding,  $dE/dz > 0$  so that we must solve  $\mathcal{Q}[z, E(z)] = 0$ . Rearranging the different terms gives :

$$\eta y^3 + y^2 - \eta \{ \kappa [1 - \ln(1 + \eta y)] + [\Omega_M + \Omega_r(1 + z)] \times (1 + z)^3 \} y + \kappa \ln(1 + \eta y) = [\Omega_M + \Omega_r(1 + z)](1 + z)^3, \quad (24)$$

where we have set  $y = E(z)$  and defined :

$$\eta = \frac{\sqrt{3\alpha}}{\varepsilon}, \quad (25)$$

$$\kappa = \frac{2\varepsilon^2}{3c_1} = -\frac{2a_0^2}{3c^2 H_0^2} \simeq -0.01 h^{-2}. \quad (26)$$

with  $h = H_0/(100/\text{km/s/Mpc})$ . Note that, in the rhs of Eq.(26), we have used Eq.(19) and set  $a_0 = 1.2 \times 10^{-10} \text{ m/s}^2$  in agreement with the estimates coming from the MOND fit to the galaxy rotation curves.

In order to reduce the number of parameters of the model, we can insert Eq.(22) into (12) and evaluate it at  $z = 0$ . Remembering that  $E(z = 0) = 1$  by definition, we then get :

$$\ln(1 + \eta) - \frac{\eta}{1 + \eta} = \frac{1 - \Omega_M - \Omega_r}{\kappa} \quad (27)$$

which can be solved numerically for given values of  $(\Omega_M, \Omega_r, h)$ . Actually, since  $\Omega_r$  is typically set by the CMB temperature, the simple MONDian vector model is fully characterized by only two parameters. This is the same as the concordance  $\Lambda$ CDM model where the same parameters  $(\Omega_M, h)$  have to be assigned in order to compare the theory with the data. However, in that scenario, two different ingredients are invoked in order to explain the dynamics of galaxies and the cosmic speed up, while here the solution to both problems comes out as a consequence of the presence of a single vector field.

### B. The standard MONDian vector model

We can repeat the same steps as before to get the master equation for the case when  $\mathcal{F}(\mathcal{K})$  is given by Eq.(23). Not surprisingly given the similarities of the models, we still get an algebraic relation :

$$2 + \kappa \eta^2 + \frac{\kappa \eta}{y \sqrt{1 + \eta^2 y^2}} - \frac{\kappa \eta^3 y}{\sqrt{1 + \eta^2 y^2}} = \frac{2[\Omega_M + \Omega_r(1 + z)](1 + z)^3 + \kappa \ln(\eta y + \sqrt{1 + \eta^2 y^2})}{y^2} \quad (28)$$

with  $y, \eta$  and  $\kappa$  defined as above. The relation between  $\eta$  and the other model parameters may be obtained as before and turns out to be :

$$\ln(\eta + \sqrt{1 + \eta^2}) - \frac{\eta(1 - \eta^2)}{\sqrt{1 + \eta^2}} = \frac{2(1 - \Omega_M - \Omega_r)}{\kappa} \quad (29)$$

which has still to be solved numerically. Note that, as for the simple case, also the standard MONDian vector model is characterized by only two quantities, namely the total matter density parameter  $\Omega_M$  and the present day scaled Hubble constant  $h$ .

## III. TESTING THE LOW REDSHIFT REGIME

Any model that aims to describe the evolution of the universe must be able to reproduce what is indeed observed. This is particularly true for the models we are considering since we are introducing a single vector field to get rid of both dark matter and dark energy. Matching the model with observations is also a powerful tool to constrain its parameters and, as an interesting byproduct, allows us to estimate some quantities common to every model (such as the age of the universe  $t_0$  and the transition redshift  $z_T$ ) to previous literature values.

As a first test, we are here interested in exploring the behaviour of our models in the low redshift regime so that we start by only considering data probing up to  $z \sim 1.5$ . To this end, we therefore maximize the following likelihood function :

$$\begin{aligned}
\mathcal{L}(\mathbf{p}) &\propto \mathcal{L}_{SNeIa}(\mathbf{p}) \\
&\times \exp \left[ -\frac{1}{2} \left( \frac{\omega_b^{obs} - \omega_b^{th}}{\delta\omega_b} \right)^2 \right] \\
&\times \exp \left[ -\frac{1}{2} \left( \frac{h_{HST} - h}{\delta h} \right)^2 \right] \quad (30)
\end{aligned}$$

where  $\mathbf{p}$  denotes the set of model parameters. Before discussing in detail the term related to the SNeIa data, we concentrate on the two Gaussian priors. The first one takes into account the constraints on the the physical baryon density  $\omega_b = \Omega_b h^2$  with

$$\omega_b^{obs} \pm \delta\omega_b = 0.0228 \pm 0.0055$$

as estimated in [30] and in agreement with what is inferred from the abundance of lighth elements [31]. The HST Key Project [32] has estimated the Hubble constant  $H_0$  using a well calibrated set of local distance scale estimators thus ending up with

$$h_{HST} \pm \delta h = 0.720 \pm 0.008$$

as a final model independent constraint.

### A. The SNeIa data

Since the first announcement [2] of the evidence of cosmic speed up, the importance of the SNeIa Hubble diagram as a probe of the universe background evolution has always been clear. It has therefore become a sort of *ground zero* for every proposed cosmological model to fit the SNeIa data. To this end, one relies on the predicted distance modulus<sup>2</sup>:

$$\mu_{th}(z, \mathbf{p}) = 25 + 5 \log \left[ \frac{c}{H_0} (1+z) r(z, \mathbf{p}) \right] \quad (31)$$

with  $r(z)$  the dimensionless comoving distance:

$$r(z, \mathbf{p}) = \int_0^z \frac{dz'}{E(z', \mathbf{p})}. \quad (32)$$

The likelihood function is then defined as

$$\begin{aligned}
\mathcal{L}_{SNeIa}(\mathbf{p}) &= \frac{1}{(2\pi)^{N_{SNeIa}/2} |C_{SNeIa}^{-1}|^{1/2}} \\
&\times \exp \left( -\frac{\Delta\mu \cdot C_{SNeIa}^{-1} \cdot \Delta\mu^T}{2} \right), \quad (33)
\end{aligned}$$

where  $N_{SNeIa}$  is the total number of SNeIa used,  $\Delta\mu$  is a  $N_{SNeIa}$ -dimensional vector with the values of  $\mu_{obs}(z_i) - \mu_{th}(z_i)$  and  $C_{SNeIa}$  is the  $N_{SNeIa} \times N_{SNeIa}$  covariance matrix of the SNeIa data. Note that, if we neglect the correlation induced by systematic errors,  $C_{SNeIa}$  is a diagonal matrix so that Eq.(33) simplifies to:

$$\mathcal{L}_{SNeIa}(\mathbf{p}) \propto \exp[-\chi_{SNeIa}^2(\mathbf{p})/2] \quad (34)$$

with

$$\chi_{SNeIa}^2(\mathbf{p}) = \sum_{i=1}^{N_{SNeIa}} \left[ \frac{\mu_{obs}(z_i) - \mu_{th}(z_i)}{\sigma_i} \right]^2 \quad (35)$$

with  $\sigma_i$  the error on the observed distance modulus  $\mu_{obs}(z_i)$  for the  $i$ -th object at redshift  $z_i$ . As input data, we use the Union SNeIa sample assembled in [33] by re-analysing with the same pipeline both the recent SNeIa SNLS [5] and ESSENCE [6] samples and older nearby and high redshift [4] datasets.

### B. How many model parameters ?

As shown by Eqs.(24) and (28), in order to determine the cosmic dynamics, one has to set the value of the present day total matter density parameter  $\Omega_M$ . On the other hand, the Gaussian prior on  $\omega_b$  in the likelihood function (30) and of the distance priors introduced later asks for discriminating between the baryons only and total matter physical densities. It is therefore worth wondering how  $\Omega_M$  and  $\Omega_b$  are related. Since our theory reduces to MOND in the low energy limit and MOND does not need any cold dark matter on the galactic scales (hence no other matter than the visible one), we could argue that  $\Omega_M = \Omega_b$  should hold. On the other hand, large amounts of missing matter are needed in order MOND to reproduce the observed phenomenology on cluster scales [34]. It was therefore postulated [35] that massive neutrinos (with  $m_\nu \sim 2$  eV) can play the role of dark mass in galaxy clusters. Moreover, solar and atmospheric neutrinos experiments [36] have shown that the three active neutrinos from the standard model of particle physics mix their flavours which is only possible if they are massive. Finally, it is also worth noting that it has been claimed [37] that a single sterile neutrino with mass in the range 4-6 eV is better suited to explain the results of the Miniboone experiment, while a 11 eV sterile neutrino has been indeed advocated [38] in order to solve the MOND problems on cluster and cosmological scales.

Massive neutrinos decoupled at  $\sim 1$  MeV and since last scattering they have been non relativistic particles so that, from a cosmological point of view, they behave exactly as matter. Assuming three families of degenerate neutrinos, the total matter density parameter will therefore read:

<sup>2</sup> We use  $\ln x$  and  $\log x$  to denote the logarithm base  $e$  and 10.

Par	$x$	$\langle x \rangle$	$x_{med}$	68% CL	95% CL
$\Omega_b$	0.13	0.12		(0.05, 0.23)	(0.02, 0.29)
$\log m_\nu$	0.24	0.40		(-0.16, 0.55)	(-0.88, 0.63)
$h$	0.700	0.700		(0.694, 0.706)	(0.689, 0.711)
$\Omega_b$	0.15	0.13		(0.07, 0.26)	(0.02, 0.31)
$\log m_\nu$	-0.09	0.35		(-1.10, 0.53)	(-2.40, 0.64)
$h$	0.700	0.700		(0.694, 0.706)	(0.688, 0.712)

TABLE I: Summary of the results of the likelihood analysis including SNeIa and Gaussian priors on  $\omega_b$  and  $h$ . The upper and lower part of the table refers to the simple and standard MONDian vector model respectively.

$$\Omega_M = \Omega_b + \frac{3m_\nu}{94h^2 \text{ eV}} \quad (36)$$

so that the number of model parameters is increased by one updating from  $(\Omega_M, h)$  to  $(\Omega_b, m_\nu, h)$ .

It is worth stressing, however, that discriminating between  $\Omega_M$  as a single quantity and  $\Omega_M$  as function of  $(\Omega_b, m_\nu, h)$  is only possible if the data at hand depend on them separately. To understand this point, let us consider the SNeIa Hubble diagram. In order to fit this dataset, we just need the dimensionless Hubble parameter  $E(z)$  which is obtained by solving, e.g., Eq.(24). To this end, we just have to set the value of  $\Omega_M$  so that all the SNeIa likelihood will be a function of  $(\Omega_M, h)$  only and we cannot set any constraint on  $(\Omega_b, m_\nu)$ . That is why we have added the Gaussian priors on  $\omega_b$  and  $h$  in order to make the likelihood explicitly dependent on  $\Omega_b$ . However, since the likelihood is mainly driven by the SNeIa term, one can forecast that the constraints on  $(\Omega_b, m_\nu)$  will be quite weak because of the degeneracy being only partially broken.

### C. Results

In order to maximize the likelihood function (30), we run a Markov Chain Monte Carlo (MCMC) algorithm to efficiently explore the parameters<sup>3</sup> space. We use a single chain with  $\sim 100000$  points reduced to  $\sim 3100$  after burn in cut and thinning. The histograms of the values of each parameter are then used to infer the median and the mean and the 68 and 95% confidence ranges summarized in Table I. The best fit parameters (i.e., the set maximizing the likelihood) for the simple MONDian vector model turns out to be:

$$(\Omega_b, \log m_\nu, h) = (0.056, 0.54, 0.70) ,$$

while the standard case gives:

$$(\Omega_b, \log m_\nu, h) = (0.050, 0.55, 0.70) .$$

For both models we get  $\chi^2_{SNeIa}/d.o.f. \simeq 1.02$  thus indicating a very good agreement. Moreover, the physical baryon density reads  $\omega_b = 0.0276$  (0.0246) for the simple (standard) model in good agreement with the observed value well within the  $1\sigma$  error, while both models predict values for  $h$  very close to the HST Key Project result. It is worth noting that a baryon only universe may be safely excluded since the reduced  $\chi^2$  values are of order 2.15 for both cases thus definitely ruling out models with no massive neutrinos.

A look at Table I shows that the constraints on both  $\Omega_b$  and  $\log m_\nu$  are quite weak. Moreover, the best fit values of both parameters radically differ from their median values. This is, however, not an unexpected result. As we have said, should the prior on  $\omega_b$  be neglected, the model should collapse into a two parameter one with  $\Omega_M$  replacing the set  $(\Omega_b, \log m_\nu)$ . The prior on  $\omega_b$  thus helps in discriminating between the two, but, from the point of view of maximizing the likelihood, it is of little help. Indeed, the only reliable constraint is on  $\Omega_M$  reading:

$$\langle \Omega_M \rangle = 0.28 \quad , \quad \Omega_{M,med} = 0.28 \quad ,$$

$$68\% \text{ CL} : (0.25, 0.31) \quad ,$$

$$95\% \text{ CL} : (0.23, 0.34) \quad ,$$

for the simple MONDian vector model and

$$\langle \Omega_M \rangle = 0.28 \quad , \quad \Omega_{M,med} = 0.28 \quad ,$$

$$68\% \text{ CL} : (0.25, 0.31) \quad ,$$

$$95\% \text{ CL} : (0.22, 0.33) \quad ,$$

for the standard case. Note that these values are in very good agreement with typical estimates from previous analyses of comparable datasets [7, 10, 33]. It is also worth noting that the results are almost fully independent on the functional expression adopted for  $\mathcal{F}(\mathcal{K})$  which is an expected consequence of the two models matching each other in order to fit the same SNeIa Hubble diagram. Provided that the above constraints on  $\Omega_M$  are met, we can choose whatever value of  $\Omega_b$  (for a given  $h$ ) and then find a corresponding  $\log m_\nu$  value giving rise to a model with a given likelihood value, i.e.  $\mathcal{L}$  depends only on  $(\Omega_M, h)$ . As a consequence, it is therefore not surprising that the constraints on  $(\Omega_b, \log m_\nu)$  are so weak.

With this caveat in mind, it is nevertheless interesting to look at the neutrino mass. Converting the constraints on  $\log m_\nu$  into constraints on  $m_\nu$  (in eV), we get:

<sup>3</sup> Note that, hereafter, we use  $\log m_\nu$  rather than  $m_\nu$  as neutrino mass parameter since this choice allows to explore a wider range.

$$\langle m_\nu \rangle = 2.3 \quad , \quad m_{\nu,med} = 2.5 \quad ,$$

$$68\% \text{ CL} : (0.7, 3.6) \quad ,$$

$$95\% \text{ CL} : (0.1, 4.2) \quad ,$$

for the simple MONDian vector model and

$$\langle m_\nu \rangle = 2.0 \quad , \quad m_{\nu,med} = 2.2 \quad ,$$

$$68\% \text{ CL} : (0.1, 3.4) \quad ,$$

$$95\% \text{ CL} : (0.0, 4.4) \quad ,$$

for the standard case. As yet stated, atmospheric and solar neutrino experiments have shown that the three families of standard model neutrinos are massive, but they are unable to put any constraints on their exact masses being only sensitive to mass squared differences. An upper limit on the mass may instead be set from the study of the tritium  $\beta$  decay. By this method, the Mainz-Troitsk experiment [39] was able to find  $m_\nu \leq 2.2$  eV. The median  $m_\nu$  values quoted above are smaller than this upper limit, while the 68 and 95% confidence ranges do indeed suggest that it is possible to fit the data equally well with still lighter neutrinos. On the other hand, it is worth stressing that such estimates rely on our assumption that three degenerate massive neutrinos are present so that their total density parameter reads  $\Omega_\nu = 3m_\nu/94h^2$ . It has, however, been claimed [37] that a single sterile neutrino with mass in the range 4-6 eV is better suited to explain the results of the Miniboone experiment. Should this be the case, the constraints above should be multiplied by three thus giving a single sterile neutrino with mass in the 95% confidence range (0.3, 12.6) eV. It is worth noting that a 11 eV sterile neutrino has been indeed advocated [38] in order to solve the MOND problems on cluster and cosmological scales. It is therefore tempting to investigate whether the results in [38] still hold for our vector models since on cluster scales both theories reduce to MOND.

The MCMC algorithm makes also possible to infer constraints on some interesting derived quantities. To this end, one just has to evaluate a given function  $f(\mathbf{p})$  for each point of the chain and then use the values thus obtained as yet done for the parameters  $\mathbf{p}$ . Table II summarizes the results for the present day deceleration parameter  $q_0$ , the transition redshift  $z_T$  obtained by solving  $q(z_T) = 0$  and the age of the universe  $t_0$  estimated as

$$t_0 = t_H \int_0^\infty \frac{dz}{(1+z)E(z)} \quad (37)$$

with  $t_H = 9.78h^{-1}$  Gyr the Hubble time.

Par	$x$	$\langle x \rangle$	$x_{med}$	68% CL	95% CL
$q_0$	-0.57	-0.58	(-0.62, -0.53)	(-0.65, -0.49)	
$z_T$	0.73	0.72	(0.65, 0.80)	(0.58, 0.88)	
$t_0$	13.71	13.70	(13.43, 14.00)	(13.18, 14.31)	
$q_0$	-0.58	-0.58	(-0.62, -0.53)	(-0.65, -0.49)	
$z_T$	0.73	0.72	(0.64, 0.81)	(0.57, 0.88)	
$t_0$	13.72	13.71	(13.42, 14.02)	(13.16, 14.29)	

TABLE II: Constraints on derived quantities ( $t_0$  in Gyr) from the chains obtained fitting the SNeIa with Gaussian priors on  $\omega_b$  and  $h$ . The upper and lower part of the table refers to the simple and standard MONDian vector model respectively.

As a first issue, let us consider the value of  $q_0$ . Its estimate is typically model dependent since it comes out as a derived quantity given a model parametrization. In order to escape this problem, one may resort to cosmographic analyses based only on Taylor expanding the scale factor. Using this approach, Cattoën and Visser [40] have found values between  $q_0 = -0.48 \pm 0.17$  and  $q_0 = -0.75 \pm 0.17$  depending on the details of the method used to fit the SNLS dataset. A similar analysis but using the GRBs as distance indicators allowed Capozziello and Izzo [41] to find values between  $q_0 = -0.94 \pm 0.30$  and  $q_0 = -0.39 \pm 0.11$  still in accordance with our estimates. A different approach has been instead adopted by Elgarøy and Multamäki [42] advocating a model independent parametrization of  $q(z)$ . Depending on the SNeIa sample used and the parametrization adopted, their best fit values for  $q_0$  range between -0.29 and -1.1 in good agreement with the estimates in Table II.

On the contrary, there is some conflict with the previous estimates of the transition redshift  $z_T$ . For instance, using the Gold SNeIa sample and linearly expanding  $q(z)$ , Riess et al. [4] found  $z_T = 0.46 \pm 0.13$  in agreement with the updated result  $z_T = 0.49_{-0.07}^{+0.14}$  obtained by Cuhna [43] using the Union sample. Although there is a possible marginal agreement within the 95% confidence range, we nevertheless consider this unsatisfactory result not a serious flaw of our models since the estimate of  $z_T$  is strongly model dependent so that it is not possible to decide whether the disagreement is with the data or with the fiducial model used to fit the data.

Finally, we note that the age of the universe is in agreement with previous estimates in the literature. Fitting the WMAP5 data and the SNLS SNeIa sample with a prior on the acoustic peak parameter gives [10]  $t_0 = 13.73 \pm 0.12$  Gyr in almost perfect agreement with the results in Table II. Moreover, the shape of the colour-magnitude diagram of globular clusters provides a model independent estimate, namely  $t_0 = 12.6_{-2.6}^{+3.4}$  Gyr [44], still in considerable good agreement with our values.

Summarizing, the very good fits to the SNeIa data and the agreement between observed and predicted derived quantities make us confident that both the simple and standard MONDian vector models successfully re-

produces the data thus being viable alternatives to the usual dark energy models in the low redshift regime.

#### IV. PROBING THE HIGH REDSHIFT REGIME

The SNeIa Hubble diagram and the Gaussian priors on  $\omega_b$  and  $h$  allow us to test the behaviour of the MONDian vector models only over the redshift range probed by these data. Considering that the farthest SN has redshift  $z \simeq 1.6$ , it is worth wondering whether the models work well for higher  $z$ . To answer this question, we change the likelihood function adding a further term:

$$\mathcal{L}(\mathbf{p}) \propto \mathcal{L}_{low}(\mathbf{p}) \times \mathcal{L}_{dp}(\mathbf{p}) \quad (38)$$

with  $\mathcal{L}_{low}(\mathbf{p})$  the likelihood term related to low redshift data given by Eq.(30), while  $\mathcal{L}_{dp}(\mathbf{p})$  is the distance priors dependent term which we detail below.

##### A. The distance priors

While SNeIa probe only the background evolution of the universe over a limited redshift range (up to  $z \simeq 1.5$ ), the CMBR anisotropy spectrum and the matter power spectrum measured by galaxy surveys make it possible to both constrain the dynamics of perturbations and test the model up to the last scattering surface. However, such a program is both theoretically difficult and computationally demanding. On the one hand, we must develop the full theory of perturbations to compute the  $\mathcal{C}_l$  coefficients of the multipole expansion of the CMBR anisotropies and the matter power spectrum  $P(k)$ . While this is yet done for the standard dark energy models, a full perturbation theory for the vector models we are considering is still to be developed. On the other hand, even for popular dark energy models, computing both the  $\mathcal{C}_l$  and  $P(k)$  represents a bottleneck for the algorithms matching data with theories. Fortunately, many features of the CMB and matter power spectra may be expressed as a function of a limited subset of quantities which are instead easy and straightforward to compute. Motivated by this consideration, it has become popular to summarize the main constraints coming from CMBR and matter power spectra in what are defined *distance priors*<sup>4</sup>.

In the analysis of the WMAP5 data [10], Komatsu et al. demonstrated that most of the information in the WMAP power spectrum may be summarized in a set of constraints on the following quantities:

- (i.) the physical baryon density:

$$\omega_b = \Omega_b h^2 \quad (39)$$

with  $\Omega_b$  the density parameter of baryons only;

- (ii.) the redshift  $z_{LS}$  to the last scattering surface that we approximate as [45]:

$$z_{LS} = 1048(1+0.00124\omega_b^{-0.738})[1+g_1(\omega_b)\omega_M^{g_2(\omega_b)}], \quad (40)$$

$$g_1(\omega_b) = \frac{0.0738\omega_b^{-0.238}}{1+39.5\omega_b^{0.763}}, \quad (41)$$

$$g_2(\omega_b) = \frac{0.560}{1+21.1\omega_b^{1.81}}, \quad (42)$$

having denoted with  $\omega_M = \Omega_M h^2$  the total matter physical density;

- (iii.) the acoustic scale [46]:

$$l_A = \frac{\pi(c/H_0)r(z_{LS})}{r_s(z_{LS})} \quad (43)$$

with  $r_s(z_{LS})$  the size of the sound horizon at the decoupling epoch given by:

$$r_s(a_{LS}) = \frac{c/H_0}{\sqrt{3}} \int_0^{a_{LS}} \frac{da}{a^2 E(a) \sqrt{1+Ra}}. \quad (44)$$

being  $a_{LS} = (1+z_{LS})^{-1}$  and  $R = 3\Omega_b/4\Omega_r$ ;

- (iv.) the shift parameter defined as [46]:

$$\mathcal{R} = \sqrt{\Omega_M} r(z_{LS}). \quad (45)$$

While this set of constraints relies on the CMBR data, none of them has to do with the matter power spectrum. To overcome this problem, Eisenstein et al. [47] introduced the *acoustic peak parameter* defined as

$$\mathcal{A} = \frac{\sqrt{\Omega_M H_0^2}}{cz_m} D_V(z_m) \quad (46)$$

where  $z_m$  is the median redshift of the galaxy survey used to extract the matter power spectrum and the *volume distance* is given by:

$$D_V(z) = \left[ \frac{cz}{H(z)} \times \frac{cr^2(z)}{H_0} \right]^{1/3}. \quad (47)$$

<sup>4</sup> Actually, not all these quantities are indeed distances. Nevertheless, the set of constraints is collectively referred to with this name since most of them are easily related to a distance.



Par	$x$	$\langle x \rangle$	$x_{med}$	68% CL	95% CL
$\Omega_b$	0.0394	0.0394	0.0394	(0.0385, 0.0404)	(0.0374, 0.0413)
$\log m_\nu$	-0.036	-0.037	-0.037	(-0.048, -0.025)	(-0.059, -0.012)
$h$	0.753	0.753	0.753	(0.749, 0.757)	(0.745, 0.761)
$\Omega_b$	0.0384	0.0384	0.0384	(0.0372, 0.0394)	(0.0363, 0.0402)
$\log m_\nu$	0.005	0.006	0.006	(-0.016, 0.025)	(-0.031, 0.041)
$h$	0.753	0.753	0.753	(0.749, 0.758)	(0.745, 0.761)

TABLE III: Summary of the results of the likelihood analysis. The upper and lower part of the table refers to the simple and standard MONDian vector model respectively.

The analysis of the correlation function of a sample of more than 46000 LRGs from the SDSS allowed Eiseinstein et al. to estimate:

$$\mathcal{A} = 0.469 \pm 0.017$$

thus offering another valuable constraint on the model parameters<sup>5</sup>. However, a more recent analysis of the seventh SDSS data release allowed Sanchez et al. [30] to measure the correlation function along both the radial and tangential directions thus allowing a more detailed treatment. Adding the CMBR data in a joint analysis, the authors then provided a new set of distance priors adding to the four quantities quoted above a new one defined as

$$G(z_m) = r(z_M) \times [E(z_m)]^{0.8}. \quad (48)$$

In order to take into account the distance priors, we introduce the following likelihood function:

$$\mathcal{L}_{dp}(\mathbf{p}) = \frac{1}{(2\pi)^{5/2} |C_{dp}|^{1/2}} \times \exp\left(-\frac{\Delta_{dp} C_{dp}^{-1} \Delta_{dp}^T}{2}\right) \quad (49)$$

where  $\Delta_{dp}$  is a five dimensional vector whose  $i$ -th element is given by  $\Delta_{dp,i} = x_{i,obs} - x_{i,th}$  with the subscript *obs* and *th* denoting the observed and theoretically predicted values. The label  $i$  runs from 1 to 5 referring, respectively, to  $\omega_b$ ,  $z_{LS}$ ,  $l_A$ ,  $\mathcal{R}$  and  $G(z_m)$ . Finally, we follow Appendix B of [30] to set the observed values and the covariance matrix of the distance priors.

## B. Fitting SNeIa and distance priors

We now run our MCMC algorithm to explore the models parameters space now maximizing the likelihood (38) taking care of both the SNeIa and distance priors

<sup>5</sup> Note that  $\mathcal{A}$  does not depend on  $h$ .

datasets. The median and mean values and 68 and 95% confidence ranges are summarized in Table III for both the simple and standard MONDian vector model. The best fit parameters, i.e. the values of  $(\Omega_b, \log m_\nu, h)$  that maximizes the likelihood, are not forced to be equal to the median values because of correlations among the parameters. Indeed, we find:

$$(\Omega_b, \log m_\nu, h) = (0.0392, -0.038, 0.753)$$

for the simple MONDian vector model, while it is:

$$(\Omega_b, \log m_\nu, h) = (0.0387, -0.001, 0.753)$$

for the standard case. Both models, however, do not offer a good performance in fitting the data. Indeed, for the best fit parameters, we get:

$$\chi_{SNeIa}^2/d.o.f = 1.32 \quad , \quad \omega_b = 0.0222 \quad , \quad z_{LS} = 1081.7 \quad ,$$

$$l_A = 300.0 \quad , \quad \mathcal{R} = 1.52 \quad , \quad G(z_m) = 1424 \quad ,$$

for the simple case and

$$\chi_{SNeIa}^2/d.o.f = 1.31 \quad , \quad \omega_b = 0.0219 \quad , \quad z_{LS} = 1082.3 \quad ,$$

$$l_A = 300.4 \quad , \quad \mathcal{R} = 1.54 \quad , \quad G(z_m) = 1424 \quad ,$$

for the standard model. It is immediately clear from the unusually high reduced  $\chi_{SNeIa}^2$  value signals that something is going wrong with fitting the SNeIa Hubble diagram. Indeed, with  $d.o.f. = N_{SNeIa} - 3 = 304$ , a reduced  $\chi_{SNeIa}^2/d.o.f. \simeq 1.3$  has just a tiny  $\sim 3 \times 10^{-5}$  probability to occur so that we can safely conclude that both models are not correctly fitting the SNeIa Hubble diagram data. This conclusion is further enforced comparing the above best fit distance priors whose median values and standard deviation<sup>6</sup> are as follows:

$$\omega_b = 0.0228 \pm 0.0055 \quad , \quad z_{LS} = 1090.1 \pm 0.9 \quad , \quad l_A = 301.6 \pm 0.7 \quad ,$$

$$\mathcal{R} = 1.701 \pm 0.018 \quad , \quad G(z_m) = 1175 \pm 21 \quad .$$

While the values of  $(\omega_b, z_{LS}, l_A)$  are in reasonable agreement, there are strong discrepancies for both the shift  $\mathcal{R}$  and the  $G(z_m)$  parameters. Considering the 68 and 95% confidence ranges in Table IV does not ameliorate the comparison so that we must conclude that the model is unable to fit both the SNeIa and distance priors dataset.

<sup>6</sup> Actually, the standard deviation is not a good estimator of the uncertainty on the distance priors because it does not take into account the correlations among them. However, it gives an idea of the discrepancy between predicted and observed values.

Par	$x$	$\langle x \rangle$	$x_{med}$	68% CL	95% CL
$\omega_b$	0.0224	0.0223	0.0223	(0.0219, 0.0229)	(0.0213, 0.0234)
$z_{LS}$	1081.6	1081.6	1081.6	(1081.1, 1082.0)	(1080.7, 1082.6)
$l_A$	299.9	299.9	299.9	(299.2, 300.5)	(298.6, 301.2)
$\mathcal{R}$	1.524	1.523	1.523	(1.519, 1.529)	(1.514, 1.533)
$G(z_m)$	1424	1424	1424	(1416, 1431)	(1407, 1439)
$\omega_b$	0.0218	0.0218	0.0218	(0.0211, 0.0223)	(0.0206, 0.0228)
$z_{LS}$	1082.6	1082.5	1082.5	(1081.8, 1083.4)	(1081.2, 1084.0)
$l_A$	300.6	300.6	300.6	(299.9, 301.4)	(299.1, 302.2)
$\mathcal{R}$	1.545	1.545	1.545	(1.543, 1.549)	(1.539, 1.551)
$G(z_m)$	1424	1424	1424	(1416, 1432)	(1409, 1439)

TABLE IV: Constraints on the predicted distance priors parameters. The upper and lower part of the table refers to the simple and standard MONDian vector model respectively.

It is worth investigating why this happens. Actually, a hint is given by noticing that the most discrepant parameters are those involving  $E(z)$  both directly, as for  $G(z_m)$ , or indirectly through an integral, as both  $\mathcal{R}$  and  $\chi_{SNeIa}^2$ . Taking the  $\Lambda$ CDM model as a comparison, we indeed find that both the simple and standard MONDian vector models systematically underestimates  $E(z)$ . As a consequence, the dimensionless comoving distance  $r(z)$  turns out to be overestimated thus leading to  $\mu(z)$  becoming increasingly higher than the concordance model prediction as the redshift increases in accordance with the result that  $\mu(z)$  is larger than  $\mu_{obs}$  for SNeIa with  $z > 1$ . This also explains why  $G(z_m)$  gets larger than observed, while the situation is different with the shift parameter. Indeed, according to Eq.(45), a larger  $r(z)$  should lead to a larger  $\mathcal{R}$ , while we observe the opposite result. This can, however, be easily explained considering that  $\mathcal{R}$  is also proportional to  $\Omega_M$  and we get :

$$\langle \Omega_M \rangle = 0.091 \quad , \quad \Omega_{M,med} = 0.091 \quad ,$$

$$68\% \text{ CL} : (0.089, 0.094) \quad ,$$

$$95\% \text{ CL} : (0.086, 0.096) \quad ,$$

for the simple MONDian vector model and

$$\langle \Omega_M \rangle = 0.095 \quad , \quad \Omega_{M,med} = 0.095 \quad ,$$

$$68\% \text{ CL} : (0.094, 0.097) \quad ,$$

$$95\% \text{ CL} : (0.092, 0.098) \quad ,$$

for the standard case. These values are much smaller than the typical  $\Omega_M \simeq 0.26$  [7, 10, 33] values obtained in literature thus explaining why our shift parameter turns out to be so small notwithstanding the higher  $r(z_{LS})$ .

Par	$x$	$\langle x \rangle$	$x_{med}$	68% CL	95% CL
$q_0$	-0.861	-0.861	-0.862	(-0.865, -0.858)	(-0.869, -0.855)
$z_T$	1.71	1.71	1.71	(1.68, 1.73)	(1.66, 1.76)
$t_0$	16.93	16.93	16.93	(16.84, 17.01)	(16.76, 17.10)
$q_0$	-0.856	-0.856	-0.856	(-0.859, -0.854)	(-0.861, -0.852)
$z_T$	1.67	1.67	1.67	(1.65, 1.68)	(1.64, 1.70)
$t_0$	16.77	16.77	16.77	(16.66, 16.87)	(16.60, 16.98)

TABLE V: Constraints on derived quantities (with  $t_0$  in Gyr). The upper and lower part of the table refers to the simple and standard MONDian vector model respectively.

For completeness, we also summarize in Table V the values of the present day deceleration parameter  $q_0$ , the transition redshift  $z_T$  and the age of the universe  $t_0$ . These results strengthen our conclusion that both models, while performing well in the low redshift regime, are actually quite poor in reproducing data probing higher  $z$ . Indeed, the values of  $q_0$  are in reasonable agreement with the results quoted in Sect. IIIC, even if our  $q_0$  values are somewhat extreme. On the contrary, there is a clear disagreement with the previous estimates of the transition redshift  $z_T$  with our results being very high (also outside the range probed by SNeIa Hubble diagram). Such a result furtherly signals that indeed the expansion rate and hence the transition from acceleration to deceleration of our models is too slow. Another evidence in favour of this interpretation is provided by  $t_0$  which turns out to be in strong disagreement with both the WMAP5 and globular clusters estimate. Indeed, Eq.(37) shows that, should we underestimate  $E(z)$ , the age of the universe turns out to be higher which is just what happens for both MONDian vector models.

### C. A problem with the models or the data ?

The large reduced  $\chi_{SNeIa}^2$  values, the disagreement between the best fit predicted and observed distance priors and the unacceptably high  $z_T$  and  $t_0$  results should make us conclude that both MONDian vector models are unable to fit both the low and high redshift data. Comparing the results in Table I and III, however, makes it evident that the two fitting procedures select very different regions of the parameter space. It is therefore worth wondering whether there is a problem with the distance priors data rather than with the models.

To this end, it is worth stressing that, although widely used in the recent literature (see, e.g., [7, 10, 33, 48, 49]), their estimate is actually model dependent. Indeed, in order to obtain their central values and covariance matrix, one first fits a given model (typically, the concordance  $\Lambda$ CDM one) to the full CMBR anisotropy and galaxy power spectra dataset using a Markov Chain Monte Carlo (MCMC) method to sample the posterior probability. This same model is then used to compute the distance

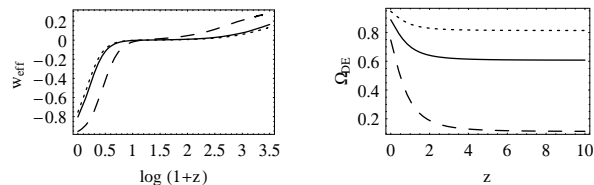


FIG. 1: Effective EoS (left) and dark energy density parameter (right) for the standard MONDian vector model. We set  $(\Omega_b, h) = (0.04, 0.70)$  and consider three values for  $\log m_\nu$ , namely -1.0 (short dashed), 0.0 (solid) and 0.5 (long dashed).

priors along the chain and then the sample thus obtained is analysed to infer the covariance matrix. As correctly stressed in [50], this procedure relies on three main assumptions:

1. the posterior probability from the CMBR anisotropies and galaxy power spectra is correctly described by the distance priors, i.e. no information is lost when giving away the full dataset in favour of the simplified one;
2. the mean and covariance matrix of the distance priors parameters do not change when the model space is enlarged, i.e. the choice of the fiducial model does not impact the estimate of the priors;
3. these summary parameters are weakly correlated with the input fiducial model parameters so that they can be used as independent constraints.

While the first and third assumptions have indeed been verified [48, 50], the second hypothesis can not be fully addressed. On the one hand, one could argue that, unless a significative amount of dark energy in the early universe is present, all reliable models should match at high redshift, when the effect of dark energy fades away. As a consequence, using the  $\Lambda$ CDM as a fiducial model to compute quantities that mainly depend on the high redshift behaviour should not affect the final estimate. However, even if the background evolution could be the same, it is still possible that the dynamics of perturbation is radically different as is the case with modified gravity theories. This is indeed what also happens for the MONDian vector models we are considering. Fixing the model parameters to the best fit values from the fit to the low redshift data only, we can easily compare the luminosity distance with that for a fiducial  $\Lambda$ CDM scenario. As expected (since they both reproduce the same data), the two can hardly be discriminated over the range probed, while the Hubble parameter only differ by a few percent. While the background evolution is therefore comparable, perturbations evolve in a completely different way because of the presence of the vector field. As such, one can not be sure that the information contained in the CMBR spectrum may still be summarized in the distance priors quantities as for the  $\Lambda$ CDM model. A similar discussion also applies for the the prior on  $G(z_m)$ . Moreover, it is

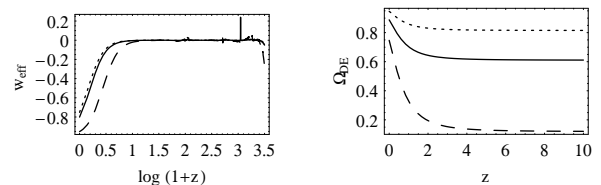


FIG. 2: Same as Fig. 1, but for the simple MONDian vector model. The small ripples are due only to numerical errors.

worth stressing that this latter quantity actually depends on data probing an intermediate redshift range so that one can not rely anymore on the fading of dark energy at high  $z$  as is typically done for quantities as, e.g., the acoustic scale  $l_A$  and the shift parameter  $\mathcal{R}$ .

Investigating the impact of these problems on the estimate of the distance priors is outside our scope here. We nevertheless stress that, because of the above considerations, one can not safely reject the MONDian vector models because of the disagreement with the distance priors values. As a conservative conclusion, we are therefore forced to only report the results being unable to decide whether the problem is with the data or with the fiducial model used to retrieve them.

#### D. The effective EoS and the high $z$ limit

An alternative way to compare the proposed MONDian vector models with standard dark energy models in both the low and high redshift regime may be obtained by considering the effective EoS. Indeed, from the point of view of the background evolution, our models are equivalent to a cosmological scenario made out of dust matter and a dark energy with an effective EoS given by:

$$1 + w_{eff}(z) = \left[ \frac{2}{3} \frac{d \ln E(z)}{d \ln(1+z)} - \frac{\Omega_M(1+z)^3}{E^2(z)} \right] \times \left[ 1 - \frac{\Omega_M(1+z)^3}{E^2(z)} \right]^{-1}, \quad (50)$$

so that the dark energy density parameter reads:

$$\Omega_{DE}(z) = \frac{1 - \Omega_M}{E^2(z)} \exp \left[ 3 \int_0^z \frac{1 + w_{eff}(z')}{1 + z'} dz' \right]. \quad (51)$$

Figs. 1 and 2 show  $w_{eff}(z)$  and  $\Omega_{DE}(z)$  for the standard and simple MONDian vector models setting the baryon density parameter to the fiducial value  $\Omega_b = 0.04$  and varying the neutrino mass  $m_\nu$ . Note that the value of  $\Omega_M$  in Eqs.(50) and (51) is related to  $\Omega_b$  and  $m_\nu$  through Eq.(36) so that changing  $m_\nu$  is the same as varying  $\Omega_M$ .

Both figures shows that the value of  $m_\nu$  set the present day EoS with  $w_{eff}(z=0)$  increasing as a function of  $m_\nu$ , even if there is a saturation at small  $m_\nu$  as can be easily understood considering that the smaller is  $m_\nu$ , the less

is the impact of massive neutrinos in the energy budget. It is worth noting that for  $\log m_\nu \simeq 0.5$ , it is  $w_{eff}(z = 0) \simeq -1.0$  and  $dw_{eff}/dz$  takes very small values over the redshift range  $(0, 1)$ , i.e. we recover (for both cases) a present day cosmological constant. It is therefore not surprising that the fit to the SNeIa dataset points towards such values of  $\log m_\nu$  since these make both MONDian vector models as similar as possible to the  $\Lambda$ CDM one over the range probed by SNeIa themselves.

On the contrary, in the high redshift regime, the neutrino mass only plays a marginal role in determining the value of  $w_{eff}(z)$  which stays almost constant at value close to the dust one  $w_{eff} = 0$ , i.e. the effective EoS approximately tracks the matter term. However, the amount of dark energy is different depending on  $m_\nu$  with lower values of the neutrino density giving rise to a larger  $\Omega_{DE}(z)$  in the high  $z$  regime. Such a behaviour is somewhat counterintuitive since one expects that the effective dark energy fades away in the early universe in order to recover the matter dominated epoch. Actually, one must take into account that our matter term is made out of baryons and massive neutrinos only. The lower is the neutrino mass, the higher must be the contribute of the effective dark energy (that in this regime behaves as matter being  $w_{eff} \simeq 0$ ) to compensate for the missing cold dark matter. Such a result can also be forecasted going back to Eq.(9) and noting that, for our best fit models, we find  $\eta \gg 1$  so that, for  $z \gg 1$ , it is  $\mathcal{K} \gg 1$  too. Let us then consider the simple MONDian vector model. Inserting Eq.(22) and taking the limit for  $\eta E(z) \gg 1$ , we approximately get :

$$\Omega_M(1+z)^3 \simeq E^2 + \ln \eta E \simeq E^2$$

so that we indeed recover the usual expression for the Hubble parameter for a matter dominated universe with  $\Omega_M$  the total (baryons and massive neutrinos) matter term (having neglected radiation). From the point of view of the effective dark energy formalism, if we reduce the neutrinos contribution, we must add a further term acting as matter and this is indeed provide by the effective dark energy. This also explains why  $\Omega_{DE}(z \gg 1)$  increases decreasing  $\log m_\nu$ . A similar discussion also applies to the standard MONDian vector models so that in both cases the final scenario is the one of a universe where the matter term disappears to be replaced by a dark energy fluid acting approximately as matter. This explains why the inclusion of the distance priors (probing the high  $z$  regime) pushes the best fit towards smaller  $\log m_\nu$  since, in this case, both MONDian models recovers the usual Friedmann models which are known to successfully fit these high redshift probes. As yet said, however, decreasing  $\log m_\nu$  makes  $w_{eff}(z = 0) \neq -1$  thus worsening the fit to the SNeIa Hubble diagram.

## V. CONCLUSIONS

The astonishing successes of MOND on the galactic scales and the emergence of a relativistic theory playing the role of its counterpart on cosmological scales have renewed the interest in the search for a possible common explanation of both dark matter and dark energy phenomenology. Vector theories are another way of recovering MOND in the low energy limit so that it is worth wondering whether they can also offer an elegant way of speeding up the cosmic evolution without the need of any dark energy source. The ignorance about the form of the vector field Lagrangian may be bypassed relying on the link between the function  $\mathcal{F}(\mathcal{K})$  and the MOND interpolating function  $\mu(a/a_0)$ . Since dark matter is no more present, one should postulate the presence of massive neutrinos in order to fill the gap between the total matter density parameter and the baryons density alone. Moreover, such massive neutrinos are also advocated in order to reconcile the results of solar and atmospheric neutrino experiments on the flavour mixing with the predictions of the standard model of particle physics.

Motivated by these considerations, we have therefore investigated the viability of two different MONDian vector models characterized by  $\mathcal{F}(\mathcal{K})$  expressions corresponding to the simple and standard MOND interpolating function. To this aim, we have first fitted them against the Union SNeIa Hubble diagram using Gaussian priors on the physical baryon density  $\omega_b$  and the present day Hubble constant  $h$  in order to break the  $(\Omega_b, \log m_\nu)$  degeneracy. Both models performs quite well giving a perfect agreement with the SNeIa data and previous estimates of the total matter density parameter  $\Omega_M$ , the deceleration parameter  $q_0$  and the age of the universe  $t_0$ . Moreover, the (weak) constraints on the neutrino mass are consistent with the upper limits set by the Mainz-Troitsk experiment assuming three families of degenerate neutrinos. Should, instead, a single sterile neutrino be the mass dominant component, its estimated mass is in agreement with the constraints from the Miniboone experiment also falling in the right range advocated to solve MOND problems on cluster scales.

In order to investigate the high redshift behaviour of the models, we have repeated the likelihood analysis adding the extended set of distance priors. It turns out that both models should be rejected since they provide now a poor fit to the SNeIa data and strongly disagree with the observed shift  $\mathcal{R}$  and  $G(z_m)$  parameters. Distance priors are, however, estimated through a model dependent procedure so that one can not safely rely on them to exclude models that are radically different from the fiducial one used to extract the constraints on  $\mathcal{R}$  and  $G(z_m)$ . As a consequence, we are unable to conclude whether the disagreement is a failure of the MONDian vector models or an expected outcome of the different evolution of perturbations with respect to usual dark energy models because of the action of the vector field.

It is worth remembering that the search for a cosmolog-

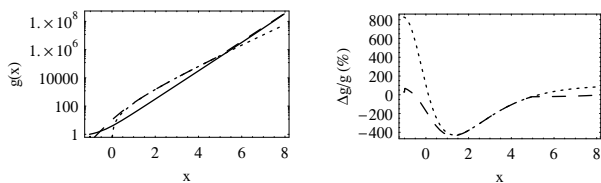


FIG. 3: *Left*: the  $g(x)$  function for the best fit standard MONDian vector model (solid line) compared to the Lue & Starkman proposals. *Right*: relative deviation of the proposal  $g(x)$  from that of our model. Short and long dashed lines refer to  $g(x)$  given by Eqs.(52) and (53) respectively.

ical counterpart to MOND has a long history with vector models being only the most recent proposal. Applying a procedure which is simply the generalization of the classical derivation of the Friedmann equation from the Newtonian force law, but now starting from the MOND force law, Lue & Starkman [51] derived an expression for the Hubble parameter without referring to any underlying modified gravity theory. Defining  $g(x) = H^2/H_0^2$  and  $x = \Omega_M(1+z)^3$ , they indeed find:

$$g(x) = \begin{cases} (\beta \ln x + c_2)x^{2/3} & x < x_c \\ x + c_1x^{2/3} & x > x_c \end{cases} \quad (52)$$

with  $c_1 = c_2 + 3\beta[\ln(3\beta) - 1]$ . Moreover, they also proposed a modified (by hand) version of this expression to better account for the low redshift behaviour:

$$g(x) = \begin{cases} \Omega_\Lambda & x \leq 0.1 \\ \beta x^{2/3} \ln(1+z) & 0.1 \leq x \leq (3\beta)^3 \\ x + 3\beta[\ln(3\beta) - 1]x^{2/3} & x > (3\beta)^3 \end{cases} \quad (53)$$

Following [51], we set  $(\beta, x_c, \Omega_\Lambda) = (15, 7 \times 10^4, 0.7)$  with  $c_2 = 0$  and show in Figs.3 and 4 how Eqs.(52) and (53) compares to the standard and simple MONDian vector models. As it is better appreciated from the right panels, both Eqs.(52) and (53) agree reasonably well with the  $g(x)$  expression of our MONDian models for very high  $x$ , that is in the early universe. This is an expected result since, in this redshift range, both our models and the phenomenological Lue & Starkman proposals recover the typical General Relativity matter dominated scenario. On the contrary, for small  $x$ , i.e. in the very low  $z$  regime, only the modified expression (53) matches reasonably well those for the standard and simple MONDian vector models as a consequence of both mimicking an effective cosmological constant. In the intermediate region, however, matching the Lue & Starkman models to our own is impossible signalling that the strategy adopted by these authors is unable to trace the transition region to General Relativity. However, it is also

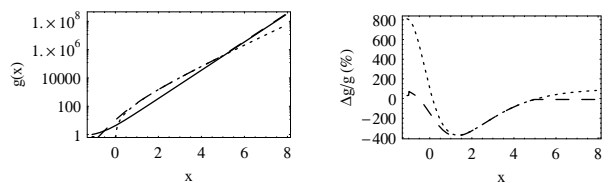


FIG. 4: Same as Fig. 3 but for the simple model.

worth stressing that such a disagreement could be expected since the Lue & Starkman procedure relies on the assumption that, whatever the underlying modified gravity theory leading to (52) or (53) is, the Birkhoff theorem still holds. This is not the case for vector theories [52] so that the two approaches differ from the very beginning.

As yet quoted in the introduction, much interest has been devoted to the TeVeS theory as a relativistic MOND counterpart. In particular, Skordis et al. [53] has also investigated the growth of structure in TeVeS also computing the CMBR anisotropy spectrum. It turned out that the inclusion of a cosmological constant term and of massive neutrinos with  $m_\nu \simeq 2$  eV may lead to a reasonably good agreement with the data, although a detailed fitting has not been performed. Since both the vector and scalar fields present in TeVeS do not contribute significantly to the dynamics, it is likely that this TeVeS +  $\Lambda$  model matches well both the SNeIa Hubble diagram and the distance priors. However, comparing the Skordis et al. model to our MONDian vector theories is not possible given the radical differences between the two approaches. Indeed, TeVeS needs the scalar field to act as a dark matter like term on galactic scales, while the vector field boosts the growth of perturbations during the  $\Lambda$  driven background expansion. On the contrary, in our approach, the vector models modify the low energy limit Poisson equation thus recovering the MOND-like behaviour, but also originates the cosmic speed up. In a sense, our approach is more *economical* claiming for the lowest possible number of ingredients.

The positive results obtained in the low redshift regime may be considered only as a ground zero level analysis. Indeed, fitting the SNeIa Hubble diagram only tells us that the two considered MONDian vector models predict the correct background evolution over the redshift range probed by the data, i.e. up to  $z \sim 1.5$ . Needless to say, more tests are needed in order to assess the viability of these models. On one hand, we can still investigate the background evolution by extending the redshift range through the use of the GRBs Hubble diagram [54]. On the other hand, a more significative and demanding test should be fitting both the galaxy power spectrum and the CMBR dataset. However, both these tasks are quite daunting from the theoretical point of view. Indeed, as far as we know, the CMBR spectrum has never been computed for the class of vector theories we are considering so that one should first write down the full set of perturbation equations to then modify a numerical code

like CAMB [55]. Somewhat easier (even if still difficult) is to deal with the problem of growth of structures in vector models. Indeed, such a study has although been performed in [56] where the authors considered a simple power-law choice for  $\mathcal{F}(\mathcal{K})$ . Although a detailed fitting to the data was not performed, these authors have convincingly shown that the new degrees of freedom sourced by the vector field may indeed boost the growth of structure even in absence of any dark matter. This result is a good starting point for testing our proposed MONDian vector models provided one accordingly changes the  $\mathcal{F}(\mathcal{K})$  function and introduces massive neutrinos into the game. Note that, since we want to recover MOND on galactic scales, we are postulating no cold dark matter so that the observed galaxy power spectrum should be matched to the predicted one with a bias parameter determined by the clustering properties of the massive (sterile or not) neutrino. Therefore, such a test is particularly powerful and worth addressing as the next step of our analysis.

It is worth noting that help investigating the viability of our MONDian vector models may come from a non astrophysical experiment. Indeed, one of the key ingredients in both MONDian vector models is the presence of massive neutrinos with  $m_\nu \sim 2$  eV. The KATRIN experiment [57] on the tritium  $\beta$  decay should be able

to constrain the electron neutrino mass with a sensitivity of  $\sim 0.2$  eV. Should this experiment indeed find that neutrinos are less massive than, e.g.,  $\sim 1$  eV, our model could be in serious trouble unless one assumes that a single massive sterile neutrino does indeed exist.

As a final remark, one could note that we have titled our paper with a question so that the reader could now claim for an answer. Unfortunately, because of the uncertainties on the use of the distance priors and the small redshift range probed, the unique answer we can give after our analysis is only a (somewhat frustrating) *maybe*.

### Acknowledgments

It is a pleasure to thank A. Sánchez for making available the covariance matrix of the distance priors in electronic form and for the illuminating comments on their use. We also warmly thank G. Angus for the instructive discussion on sterile neutrinos in MOND, and A. Diaferio and A. Tartaglia for a careful reading of the manuscript. VFC is supported by University of Torino and Regione Piemonte. Partial support from INFN project PD51 is acknowledged too.

- 
- [1] Y. Sofue, V. Rubin, *ARA&A*, 39, 127, 2001
- [2] S. Perlmutter et al., *ApJ*, 483, 565, 1997; A.G. Riess et al., *AJ*, 116, 1009, 1998; B.P. Schmidt et al., *ApJ*, 507, 46, 1998; P.M. Garnavich et al., *ApJ*, 509, 74, 1998; S. Perlmutter et al., *ApJ*, 517, 565, 1999
- [3] R.A. Knop et al., *ApJ*, 598, 102, 2003; J.L. Tonry et al., *ApJ*, 594, 1, 2003; B.J. Barris et al., *ApJ*, 602, 571, 2004
- [4] A.G. Riess et al., *ApJ*, 607, 665, 2004; A.G. Riess et al., *ApJ*, 659, 98, 2007
- [5] P. Astier et al., *A&A*, 447, 31, 2006
- [6] W.M. Wood-Vasey et al., *ApJ*, 666, 694, 2007
- [7] T. Davis et al., *ApJ*, 666, 716, 2007
- [8] P. de Bernardis et al., *Nature*, 404, 955, 2000; R. Stompfer et al., *ApJ*, 561, L7, 2001; C.B. Netterfield et al., *ApJ*, 571, 604, 2002; R. Rebolo et al., *MNRAS*, 353, 747, 2004
- [9] C.L. Bennett et al., *ApJS*, 148, 1, 2003; D.N. Spergel et al., *ApJS*, 148, 175, 2003 D.N. Spergel et al., *ApJS*, 170, 377, 2007
- [10] E. Komastu et al. 2009, *ApJS*, 180, 330, 2009
- [11] S. Dodelson et al., *ApJ*, 572, 140, 2002; W.J. Percival et al., *MNRAS*, 337, 1068, 2002; A.S. Szalay et al., *ApJ*, 591, 1, 2003; E. Hawkins et al., *MNRAS*, 346, 78, 2003; A.C. Pope et al., *ApJ*, 607, 655, 2004
- [12] S.M. Carroll, W.H. Press, E.L. Turner, *ARAA*, 30, 499, 1992; V. Sahni, A. Starobinski, *Int. J. Mod. Phys. D*, 9, 373, 2000
- [13] M. Tegmark et al., *Phys. Rev. D*, 69, 103501, 2004; U. Seljak et al., *Phys. Rev. D*, 71, 043511, 2005; M. Tegmark et al., *Phys. Rev. D*, 74, 123507, 2006
- [14] P.J.E. Peebles, B. Rathra, *Rev. Mod. Phys.*, 75, 559, 2003; T. Padmanabhan, *Phys. Rept.*, 380, 235, 2003; E.J. Copeland, M. Sami and S. Tsujikawa, *Int. J. Mod. Phys. D*, 15, 1753, 2006
- [15] G.R. Dvali, G. Gabadadze, M. Porrati, *Phys. Lett. B*, 485, 208, 2000; G.R. Dvali, G. Gabadadze, M. Kolanovic, F. Nitti, *Phys. Rev. D*, 64, 084004, 2001; G.R. Dvali, G. Gabadadze, M. Kolanovic, F. Nitti, *Phys. Rev. D*, 64, 024031, 2002; A. Lue, R. Scoccimarro, G. Starkman, *Phys. Rev. D*, 69, 044005, 2004; A. Lue, R. Scoccimarro, G. Starkman, *Phys. Rev. D*, 69, 124015, 2004
- [16] I. Fujii, K. Maeda, *The scalar-tensor theory of gravity*, Cambridge University Press, Cambridge (UK), 2003
- [17] S. Capozziello, M. Francaviglia, *Gen. Rel. Grav.*, 40, 357, 2008 T.P. Sotiriou, V. Faraoni, preprint arXiv:0805.1726, 2008
- [18] T. Jacobson, D. Mattingly, *Phys. Rev. D*, 64, 024028, 2004; B.Z. Foster, T. Jacobson, *Phys. Rev. D*, 73, 064015, 2006; C. Eling, *Phys. Rev. D*, 73, 104012, 2006
- [19] J. Bekenstein, *Phys. Rev. D*, 70, 083509, 2004
- [20] T.G. Zlosnik, P.G. Ferreira, G.D. Starkman, *Phys. Rev. D*, 74, 044037, 2006
- [21] T.G. Zlosnik, P.G. Ferreira, G.D. Starkman, *Phys. Rev. D*, 75, 044017, 2007
- [22] S.M. Carroll, E.A. Lim, *Phys. Rev. D*, 70, 123525, 2004
- [23] C. Heinicke, P. Baekler, F.W. Hehl, *Phys. Rev. D*, 72, 025012, 2005
- [24] R.H. Sanders, S.S. McGaugh, *Ann. Rev. Astron. Astroph.*, 40, 263, 2002
- [25] B. Famaey, J. Binney, *MNRAS*, 363, 603, 2005
- [26] J. Bekenstein, M. Milgrom, *ApJ*, 286, 7, 1984
- [27] H.S. Zhao, B. Famaey, *ApJ*, 638, L9, 2006; B. Famaey, J.Ph. Bruneton, H.S. Zhao, *MNRAS*, 377, L79, 2007; R.H. Sanders, E. Noordermeer, *MNRAS*, 379, 702, 2007; G.W. Angus, B. Famaey, O. Tiret, F. Combes, H.S. Zhao,

- MNRAS, 383, L1, 2008
- [28] E.A. Lim, Phys. Rev. D, 71, 063504, 2005
- [29] C. Eling, T. Jacobson, D. Mattingly, *Einstein - Aether theory*, in *Deserfest: A Celebration of the Life and Works of Stanley Deser*, Ann Arbor, Michigan, apr 2004
- [30] A.G. Sánchez, M. Crocce, A. Cabré, C.M. Baugh, E. Gaztañaga, preprint arXiv 0901.2570, 2009
- [31] D. Kirkman, D. Tyler, N. Suzuki, J.M. O'Meara, D. Lubin, ApJS, 149, 1, 2003
- [32] W.L. Freedman et al., ApJ, 553, 47, 2001
- [33] M. Kowalski et al., ApJ, 686, 749, 2008
- [34] A. Aguirre, J. Schaye, E. Quataert, ApJ, 561, 550, 2001; E. Pointconteau, J. Silk, MNRAS, 364, 654, 2005; D. Clowe et al., ApJ, 648, L109, 2006; G.W. Angus, H.Y. Shawn, H.S. Zhao, B. Famaey, ApJ, 654, L13, 2007; G.W. Angus, B. Famaey, D.A. Buote, MNRAS, 387, 1470, 2008
- [35] R.H. Sanders, MNRAS, 342, 901, 2003; R.H. Sanders, MNRAS, 380, 331, 2007
- [36] Q.R. Ahmad et al., Phys. Rev. Lett., 87, 071301, 2001; Y. Ashie et al., Phys. Rev. Lett., 93, 101801, 2004
- [37] A. Aguilar et al., Phys. Rev. D, 64, 112007, 2001; M. Maltoni, T. Schwetz, Phys. Rev. D, 76, 093005, 2007; C. Giunti, M. Laveder, Phys. Rev. D, 77, 093002, 2008
- [38] G.W. Angus, MNRAS, 394, 527, 2009; G.W. Angus, B. Famaey, A. Diaferio, in preparation, 2009
- [39] C. Kraus et al., Eur. Phys. J. C, 40, 447, 2005
- [40] C. Cattoën, M. Visser, Phys. Rev. D, 78, 063501, 2008
- [41] S. Capozziello, L. Izzo, A&A, 490, 31, 2008
- [42] O. Elgarøy, T. Multamäki, JCAP, 09, 002, 2006
- [43] J.V. Cunha, Phys. Rev. D, 79, 047301, 2009
- [44] L. Krauss and B. Chaboyer, Science, Jan 3 2003 issue
- [45] W. Hu, N. Sugiyama, ApJ, 471, 542, 1996
- [46] J.R. Bond, G. Efstathiou, M. Tegmark, MNRAS, 291, L33; G. Efstathiou, J.R. Bond, MNRAS, 304, 75, 1999; L. Page et al., ApJS, 144, 233, 2003
- [47] D.J. Eisenstein, ApJ, 633, 560, 2005
- [48] Y. Wang, P. Mukherjee, Phys. Rev. D, 76, 103533, 2007;
- [49] O. Elgarøy, T. Multamäki, A&A, 471, 65, 2007; E.L. Wright, ApJ, 664, 633, 2007; R. Lazkoz, S. Nesseris, L. Perivolaropoulos, JCAP, 7, 12, 2008
- [50] R. Biswas, B.D. Wandelt, preprint arXiv:09032532, 2009
- [51] A. Lue, G.D. Starkman, Phys. Rev. Lett., 92, 131102, 2004
- [52] C. Eling, T. Jacobson, Class. Quant. Grav., 23, 5625, 2006; T. Jacobson, Class. Quant. Grav., 24, 5719, 2007
- [53] C. Skordis, D.F. Mota, P.G. Ferreira, C. Boehm, Phys. Rev. Lett., 96, 011301, 2006
- [54] B.E. Schaefer, ApJ, 660, 16, 2007; V.F. Cardone, S. Capozziello, M.G. Dainotti, preprint arXiv:0901.3194, 2009
- [55] A. Lewis, A. Challinor, A. Lasenby, ApJ, 538, 473, 2000
- [56] T.G. Zlosnik, P.G. Ferreira, G.D. Starkman, Phys. Rev. D, 77, 084010, 2008
- [57] J. Angrik et al., FZK Scientific Report, 7090, 2005; see also <http://www-ik.fzk.de>